

Diffuse interface modeling of eggplants vacuum freeze-drying process

*Original*

Diffuse interface modeling of eggplants vacuum freeze-drying process / Bobba, S., Harguindeguy, M., Colucci, D., Fissore, D.. - ELETTRONICO. - (2019), pp. 29-35. (7th European Drying Conference Torino, Italy July 10-12).

*Availability:*

This version is available at: 11583/2739532 since: 2020-01-08T11:32:06Z

*Publisher:*

Politecnico di Torino

*Published*

DOI:

*Terms of use:*

This article is made available under terms and conditions as specified in the corresponding bibliographic description in the repository

*Publisher copyright*

(Article begins on next page)

## DIFFUSE INTERFACE MODELING OF EGGPLANT VACUUM FREEZE-DRYING PROCESS

*Serena Bobba, Maitê Harguindeguy, Domenico Colucci, Davide Fissore*

Dipartimento di Scienza Applicata e Tecnologia, Politecnico di Torino  
Corso Duca degli Abruzzi 24, 10129 Torino, Italy  
Email: serena.bobba@polito.it

### Abstract

Vacuum freeze-drying (VFD) can be used for preserving food with small effects on nutritional qualities. VFD modelling is useful to select off-line the best operating conditions to avoid product overheating and reduce the drying time, thus saving energy. A 3D diffuse interface model was developed to simulate *in-silico* eggplant VFD. By comparing the experimental drying time and product temperature, heat transfer coefficient and vapor diffusivity were estimated under different operating conditions.

**Keywords:** modelling, vacuum freeze-drying, diffuse interface, kinetic, eggplant.

### 1. Introduction

Vacuum freeze-drying (VFD) is a low pressure and low temperature drying process based on sublimation as the water removal mechanism. Since a high-water content favours a series of degradation reactions and microbial growth, freeze-drying can be applied to food products as a preservation process. In comparison to other drying processes, VFD is less damaging in terms of aesthetic and nutritional product qualities, thanks to the low temperature along the whole process and the low oxygen concentration in the atmosphere.

Unfortunately, the process is time and energy consuming, and attention should be paid in the choice of process variables, i.e. temperature of the heating shelves and chamber pressure, to preserve product quality and minimizing the process duration. Therefore, it is really useful to perform *in silico* simulations of the sublimation process to select temperature and pressure values that allow a complete drying in a shorter time, while avoiding product overheating.

Two layers can be found in the product while the sublimation occurs: an external dried layer and a frozen inner core, which gets smaller over time as the sublimation goes on. To take this into account, several models were developed, based on the Uniformly Retreating Ice Front (URIF) (Wolff and Gibert, 1990) approach. URIF models consider each cell of the computational domain made of pure ice or pure dried matrix and the interface between the two parts of the product moves from the exterior to the interior of the system. Such approach is particularly useful for one-dimensional systems.

However, the gradients of temperature and compositions created during the drying may be different in the three dimensions, e.g. due to non-uniform heating conditions, and the adoption of a one-dimensional model is a simplification that may lead to information loss on the real evolution of the system. Thereby, a three-dimensional (3D) model seems more appropriate to describe accurately a 3D domain where there are significant three-dimensional gradients. According to the URIF approach, the deformation over time of the sublimation interface requires a computational grid rearrangement to fit the shape of the sublimation front. This grid rearrangement is computationally critical in case it has to reshape the sublimation interface over three directions, making the URIF approach not convenient for a 3D system.

Warning *et al.* proposed a Diffuse Interface model (DIM) (Warning *et al.*, 2015) in order to keep the same computation grid for all the calculations. This is achieved thanks to the innovative description of the product composition. Each cell of the grid is composed by a constant solid fraction,



considered as a solid matrix, plus a fraction of water, which occupies the volume left by the solid matter, i.e. it occupies the porosity inside the solid matrix. The water contained in the porosities can be found as ice or vapor, according to the sublimation front evolution during the drying phase. Consequently, the porosity composition is time varying, made of the sum of ice fraction ( $S_i$ ) and vapor ( $S_g$ ).

While the sublimation interface of URIF models is defined by the sharp boundary between ice and dried cells, the sublimation interface of a DIM is implicitly described by the position of cells whose ice fraction is being equal to zero. Conceptually, in the first, sublimation is happening only at the sharp boundary while in the second approach sublimation is happening throughout the domain.

The goal of this study was to develop a mathematical model, applying the DIM approach, to describe the evolution of product temperature and of the residual amount of ice during the primary drying, thus estimating the time required to complete this phase. The case study considered is the freeze-drying of eggplant samples, *Solanum melongena* variety, a challenging case study due to the high-water content and soft texture of the solid matrix.

In this framework, applying a DIM may be useful to take into consideration the occurrence of 3D gradients in the samples, since the product is strongly affected by external conditions at the surface. In particular, during the drying phase the product is heated both from the shelf and from chamber walls, whose temperature is typically higher than that of the product. It is well known that radiative heat from the walls to the products exposed on the shelves is significant and may play a major role in determining the product temperature (Rambhatla and Pikal, 2004). Therefore, radiative heat is responsible for the higher temperature at the product surface, thus leading to considerable temperature gradients in the product that may be not negligible for a deep analysis of the product being processed.

## 2. Material and method

### 2.1 Mathematical model

The mathematical model here presented consists of a differential equations system, developed from the DIM presented by Warning *et al.* (Warning *et al.*, 2015), implemented by applying a Finite Element Method.

Some assumptions were taken into account to simulate the system. Firstly, any shrinkage phenomena are neglected, as no evidences of it were reported experimentally. Therefore, the modelled geometric shape considered is cubic and constant with time. This approach required a description of the analytical domain, i.e. the product with a cubic three-dimensional grid. Thanks to the DIM approach, the same set of equations presented can be applied to all the domain cells, as long as some effective proprieties are used. These properties are average properties, weighted by the cell composition in terms of solid, ice, and vapor fractions (Warning *et al.*, 2015).

The ice sublimation flux ( $\dot{I}$ , kg s<sup>-1</sup> m<sup>-3</sup>) was described by the non-equilibrium formulation reported in equation (1), where  $\phi$  is the porosity,  $M_w$  (kg mol<sup>-1</sup>) is the molecular weight of water and  $R$  (J mol<sup>-1</sup> K<sup>-1</sup>) the ideal gas constant. This means that the phase change of ice into vapor takes place rapidly, but not instantaneously. Equation 1 points out that the sublimation can occur as long as the ice vapor pressure ( $Pv_i$ ) is higher than the chamber pressure ( $P_c$ ) and the volume fraction of gas ( $S_g$ ) is not zero. The non-equilibrium constant ( $K_{eq}$ , s<sup>-1</sup>) is representative of the sublimation rate. To ensure that the sublimation is not rate controlled by the phase change,  $K_{eq}$  is set as a large value in the order of 10<sup>5</sup>-10<sup>6</sup> s<sup>-1</sup>. Thereby, the phase change takes place in a much smaller time scale than the vapor diffusion phenomena through the porous matrix, which should be the actual process rate controlling.

$$\dot{I} = K_{eq} (Pv_i - P_c) \frac{M_w \phi S_g}{RT} \quad (1)$$

The mass balance of water vapor through the porous matrix is shown in equation (2), where  $\rho_g$  is the vapor density,  $\rho_i$  the ice density, and  $S_i$  the volume fraction of ice. The vapor flux takes place thanks to the vapor gradient from the product to the chamber. This is taken into account by the vapor diffusivity ( $D_{eff}$ , m<sup>2</sup> s<sup>-1</sup>) and occurs through the solid matrix by means of diffusive phenomena.

$$\frac{d\rho_g}{dt} = \frac{1}{\phi(1-S_i)} \left( -\frac{\rho_g}{\rho_i} \dot{i} + D_{eff} \nabla^2 \rho_g + \dot{i} \right) \quad (2)$$

The vapor flow regime in the porous medium can be affected by some deviation from the continuum assumption. In fact, in case the Knudsen number ( $K_n$ ), used to establish in which regime the flow takes place, is higher than 1, Knudsen diffusivity should be considered. If the pore diameter is assumed as the characteristic length, in the order of 1-100  $\mu\text{m}$ ,  $K_n$  can be much higher than 1 (Warning *et al.* 2015). However, the Knudsen diffusivity that should be introduced is related to the effective diffusivity by the void fraction and the tortuosity of the porous matrix (Fissore *et al.*, 2015). Because of the uncertainty on these parameters,  $D_{eff}$  was estimated from experimental data fitting. The heat balance implemented can be seen in equation (3), where  $\rho_{eff}$  ( $\text{kg m}^{-3}$ ),  $Cp_{eff}$  ( $\text{J kg}^{-1} \text{K}^{-1}$ ) and  $k_{eff}$  ( $\text{W m}^{-1} \text{K}^{-1}$ ) are respectively the effective density, heat capacity and conductivity of the product,  $\lambda$  ( $\text{J kg}^{-1}$ ) is the ice latent heat of sublimation:

$$\frac{dT}{dt} = \frac{1}{\rho_{eff} Cp_{eff}} (k_{eff} \nabla^2 T - \lambda \dot{i}) \quad (3)$$

## 2.2 Boundary and initial conditions

In order to solve partial differential equations (PDE) system made of equations (1) and (3), boundary and initial conditions about temperature and gas density are required.

The initial sample temperature ( $T_0$ ) was the product temperature at the end of the freezing stage, equal to  $-30^\circ\text{C}$  in the case study analysed. The initial gas density ( $\rho_{g0}$ ) was calculated by assuming ideal gas behaviour, thanks to the low pressure at vacuum conditions and considering vapor to be the only gas in the chamber.

The boundary conditions regarding temperature were developed considering that the product is heated both from the shelf and from the chamber walls, which are at higher temperature.

Firstly, the sample is heated by the shelf through the bottom face by a heating flux proportional to the difference between the shelf temperature and the product, multiplied by the heat transfer coefficient ( $K_v$ ,  $\text{W m}^{-2} \text{K}^{-1}$ ). This is an overall coefficient taking into account the heating mechanisms occurring between shelf and the bottom face of the cube.

From the other five faces exposed to the chamber, the cubic sample is heated by radiation from the chamber walls. In order to compute the radiative heat, it is required to know the view factors values and the effective emissivity ( $\epsilon$ ). The latter depends on the emissivity of the involved surfaces, thus on the specific material (Pikal *et al.*, 1984), and a value of 0.98 was adopted. For the view factors, many approximations were needed to estimate them, as an exact evaluation would be computationally too complex. Therefore, only the most significant contributions given by some of the areas of the chamber walls were considered (Fig. 1). The other ones were characterized by much lower view factors, which minimize their contribution to the heat radiated. In particular, the upper face of the cube was considered to be irradiated by the upper shelf surface and by the four chamber walls, while each side of the cube was considered to be irradiated by the corresponding shelf parallel to the side surface, from an area as large as the cube's side itself, since this corresponds to the actual disposition of samples on the shelf adopted in the batches from which experimental data were collected.

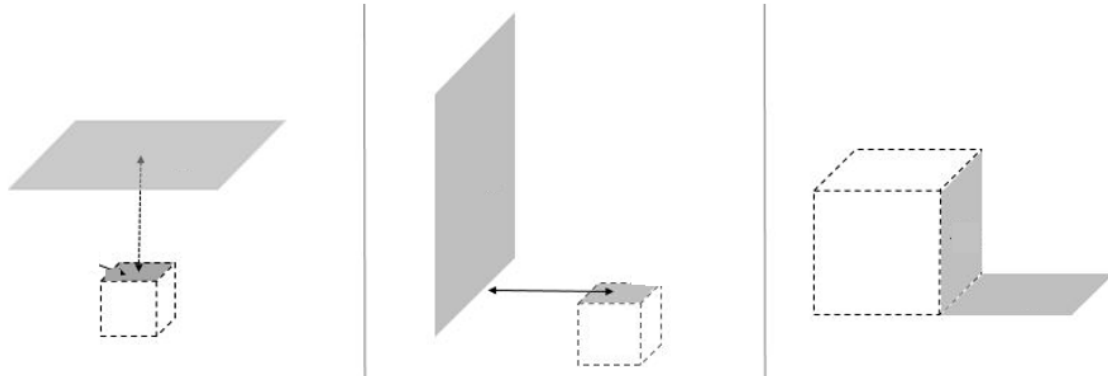


*Fig. 1. Representation of the geometrical configuration considered to calculate the view factors. On the left and in the middle, the upper shelf and the chamber wall radiate the upper product face. On the right, the side product face being radiated by an area of the shelf equal to the product face area.*

The boundary conditions regarding the gas density considers the vapor diffusion from the product surface to the chamber.

The diffusive vapor flux ( $\dot{Q}_D$ ,  $\text{kg s}^{-1} \text{m}^{-2}$ ) boundary condition from the surface to the chamber was the one implemented by equation (4) for the five exposed faces, each one of area equal to  $A$  ( $\text{m}^2$ ). The vapor propagates through the porous matrix to the surface, and then through the vacuum chamber. The vapor propagation in these different materials is characterized by different diffusivities, and this should be considered for setting the boundary condition in equation (4). Since the diffusivity of vapour in the chamber can be hardly calculated because of the environment conditions under vacuum, an approach analogue to the ghost cells one was adopted. Ghost cells represent a shell of cells around the product, that can be characterized with specific properties values (Mittal and Iaccarino, 2005). In this study, the ghost cells were considered as a layer around the product where the vapor diffusivity is the same as inside the porous matrix, thus allowing the use of a single parameter. Since the contact with the shelf might prevent diffusive phenomena, the face laying on the shelf was assumed impermeable to the vapor flux and, thus,  $\dot{Q}_D$  through in this case was assumed to be equal to zero.

$$\dot{Q}_D = -\frac{D_{eff}}{A}(\rho_{ext} - \rho_g) \quad (4)$$

## 2.3 Experimental Investigation

Data collected on freeze dried eggplant samples were used to develop the present model. Fresh eggplants were bought in a local market in Turin and processed daily. This product is highly heterogeneous, due to the high seasonal variability and differences between each cultivar. Furthermore, the eggplant samples composition is not homogeneous due to the presence of seeds in the vegetable flesh, affecting the data collected.

Eggplants were freeze-dried in a LyoBeta 25 by Telstar (Terrassa, Spain), which is a pilot-scale equipment with  $0.2 \text{ m}^3$  chamber volume. Temperature profiles and drying duration were measured in batches run at different conditions.

To monitor the product superficial temperature an infrared thermography-based sensor (FILR A35) was used (Lietta et al., 2018), while the temperature inside the samples was measured by means of thermocouples (Tersid, Milano, Italy).

For estimating the end point of the drying phase, pressure measurements were taken by a Pirani (PP) gauge (PSG-101-S, Inficon, Bad Ragaz, Switzerland) and a capacitive one (PB), both installed in the chamber. Their ratio (PP/PB) decrease was regarded as an evidence for end of drying (Patel et al., 2010). In particular, in this study, the middle point of the decreasing curve was considered as a representative end point.

## 3. Results and discussion

In order to model product temperature and drying duration, estimating first the values of  $K_v$  and  $D_{eff}$  was required for describing the heat and mass transfer. The comparison between experimental and simulated data was focused on the product surface temperature and the drying process duration. In fact, the former parameter is crucial for preserving food nutritional properties, since higher temperatures may affect these properties while also having an impact on process duration. The latter is relevant for optimizing the process duration. In particular, the simulated drying duration was calculated as ice ratio, i.e. the fraction of residual ice mass over the initial one.

By comparing three temperature profiles at the product surface with the modelled ones, as well as the drying time, it was possible to estimate  $K_v$  and  $D_{eff}$  values under conditions of  $-30^\circ\text{C}$  and  $30\text{ Pa}$  (case A). Following,  $K_v$  and  $D_{eff}$  mean values were calculated, as well as their standard deviations, equal to  $28.4\text{ W m}^{-2}\text{ }^\circ\text{C}^{-1}$  and  $2.7\cdot 10^{-4}\text{ m}^2\text{ s}^{-1}$ . The model validity was proved by comparing calculated and measured temperature evolution in another sample, taken from the batch at same conditions, by employing the  $K_v$  and  $D_{eff}$  mean values (Fig. 2).

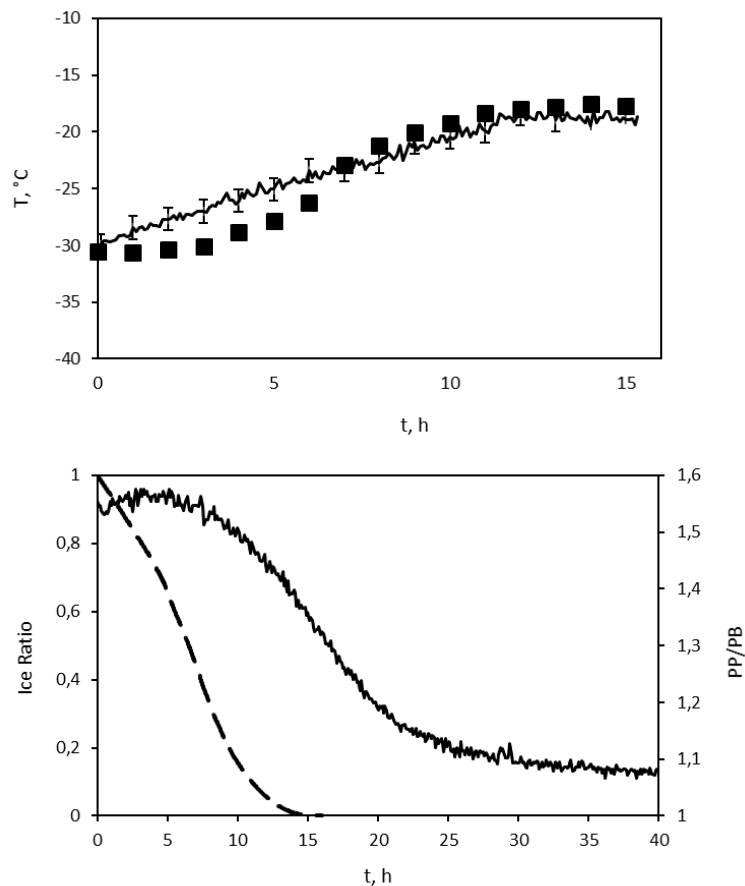
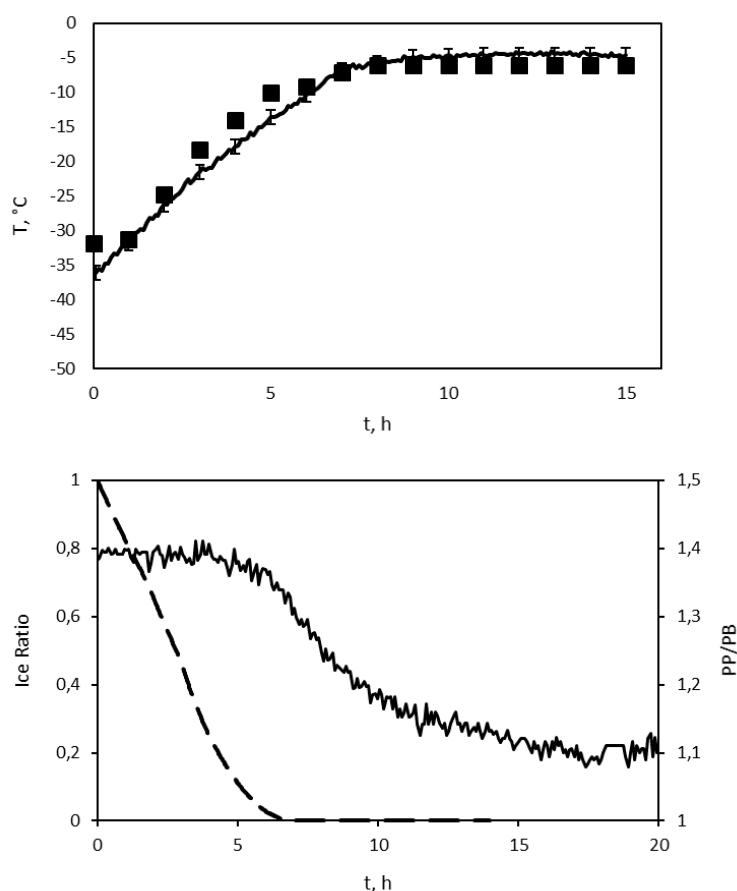


Fig. 2. Above, experimental temperature profile of the product surface dried at  $-30^\circ\text{C}$  and  $30\text{ Pa}$ , compared to the one calculated (■) with the  $K_v$  and  $D_{eff}$  mean values to verify the model accuracy. Below, comparison of the experimental PP/PB ratio (on the right axes) and the simulated ice ratio (dashed, on the left axes) for the same case study.

The presented model appears to adequately fit the temperature trends, with particular accuracy in the last hours of drying, when the sublimation is being completed. Regarding the drying time, it can be seen that the modelled drying is completed at a time very close to the experimental one.

Furthermore, the model was applied to the data collected in a batch run at  $-15^\circ\text{C}$  and  $20\text{ Pa}$  (case B), to check if it could be applied under different process conditions. In this case, the values found to give a good data fitting (Fig. 3) were equal to  $14\text{ W m}^{-2}\text{ }^\circ\text{C}^{-1}$  and  $1.9\cdot 10^{-4}\text{ m}^2\text{ s}^{-1}$ .



*Fig. 3. Above, temperature profile of the product surface dried at  $-15^{\circ}\text{C}$  and 20 Pa, compared the profile modelled (■). Below, comparison of the experimental PP/PB ratio (on the right axes) and the simulated ice ratio (dashed, on the left axes) for the same case study.*

These results remark that the values of  $K_v$  and  $D_{eff}$  are influenced by temperature and pressure conditions. Since in this case both the process variables were varied, only the effect on  $K_v$  is feasible, as it is well known that  $K_v$  is mainly a function of pressure (Pisano *et al.*, 2011). Therefore, in case B, the effect of a decrease in pressure results in a decrease of the heat transfer coefficient. On the other hand, the diffusivity value appears mainly constant, and the little decrease may be related to the lower chamber pressure. In fact, this is an effective value depending on the pressure difference between the chamber and ice pressure at the product interface.

#### 4. Conclusions

Vacuum freeze-drying is an interesting process to preserve food through water removal, as it allows to preserve more nutritional properties rather than other drying processes occurring at higher temperature. However, process variables have to be carefully selected to minimize the drying duration and avoid unexpected higher temperature of the product. For these purposes, modelling the drying phase of a freeze-drying cycle can be useful.

A Diffusive Interface model (DIM) was implemented, applied to a 3D domain, for simulating the drying process of eggplant, an interesting product thanks to its high-water content and good nutritional properties.

The aim of the model was simulating the temperature profile on the product surface and estimating the drying time. To achieve these goals, experimental data were fit, to estimate the values of the mass and heat transfer coefficients.

## References

- Fissore D., Pisano R., Barresi A. A., 2015, Using Mathematical Modeling and Prior Knowledge for QbD in *Freeze-Drying Processes*, (F.Jameel et al., Eds.), Chap. 23. Springer Science, New York, USA, pp. 565-593.
- Lietta E., Colucci D., Distefano G., Fissore D., 2018, On the Use of Infrared Thermography for monitoring a Vial Freeze-Drying Process., *J. Pharm. Sci.*, **108**(1), 391–398.
- Mittal R., Iaccarino G., 2005, Immersed Boundary Methods, *Annu. Rev. Fluid Mech.*, **37**(1), 239-261.
- Patel S. M., Doen T., Pikal M. J., 2010, Determination of End Point of Primary Drying in Freeze-Drying Process Control, *AAPS PharmSciTech.*, **11**(1), 73–84.
- Pikal M. J., Roy M. L., Shah S., 1984, Mass and Heat Transfer in Vial Freeze-drying of Pharmaceuticals: Role of the Vial, *J. Pharm. Sci.*, **73**(9), 1224–1237.
- Pisano R., Fissore D., Barresi A.A., 2011, Heat Transfer in Freeze-drying Apparatus in *Heat Transfer* (B. Dos Santos, Ed.), Chap. 6, Tech Open Access Publisher, Rijeeka, Croatia, pp. 91-114.
- Rambhatla S., Pikal M., 2004, Heat and Mass Transfer Scale-up Issues During Freeze-Drying, I: Atypical Radiation and the Edge Vial Effect, *AAPS PharmaSciTech*, **4**(2), 22-31.
- Warning A. D., Arquiza J. M. R., Datta A. K., 2015, A Multiphase Porous Medium Transport Model with Distributed Sublimation Front to Simulate Vacuum Freeze Drying, *Food Bioprod. Process.*, **94**(August), 637–648.
- Wolff E., Gibert H., 1990, Atmospheric Freeze-Drying Part 2 : Modelling Drying Kinetics Using Adsorption Isotherms., *Drying Technol.*, **8**(2), 405–428.